CD133+ neural stem cells in the ependyma of mammalian postnatal forebrain

Volkan Coskun*†‡, Hao Wu†‡, Bruno Blanchi*‡, Sean Tsao†‡, Kevin Kim†‡, Jing Zhao†‡, Juan Carlos Biancotti*‡, Leah Hutnick§, Richard C. Krueger, Jr.¶∥, Guoping Fan§, Jean de Vellis*‡, and Yi E. Sun*†‡**

*Mental Retardation Research Center and Departments of †Molecular and Medical Pharmacology, ‡Psychiatry and Behavioral Sciences, and §Human Genetics, David Geffen School of Medicine, University of California, 635 Charles E. Young Drive South, Los Angeles, CA 90095; and ¶Department of Pediatrics, Cedars–Sinai Medical Center, 8700 Beverly Boulevard, Los Angeles, CA 90048

The postnatal forebrain subventricular zone (SVZ) harbors stem cells that give rise to olfactory bulb interneurons throughout life. The identity of stem cells in the adult SVZ has been extensively debated. Although, ependymal cells were once suggested to have stem cell characteristics, subsequent studies have challenged the initial report and postulated that subependymal GFAP+ cells were the stem cells. Here, we report that, in the adult mouse forebrain, immunoreactivity for a neural stem cell marker, prominin-1/CD133, is exclusively localized to the ependyma, although not all ependymal cells are CD133+. Using transplantation and genetic lineage tracing approaches, we demonstrate that CD133+ ependymal cells continuously produce new neurons destined to olfactory bulb. Collectively, our data indicate that, compared with GFAP expressing adult neural stem cells, CD133+ ependymal cells represent an additional—perhaps more quiescent—stem cell population in the mammalian forebrain.

adult neural stem cells | subventricular zone

The adult mammalian brain harbors new neurons throughout life in two discrete locations: hippocampus and subventricular zone (SVZ) [also referred to as subependymal zone (SEZ)] (1–4). Immature neurons generated in the SVZ travel along the rostral migratory stream (RMS) and become postmitotic interneurons in the olfactory bulb. The identity of the stem cells in the adult SVZ has been debated extensively. Glial fibrillary acidic protein (GFAP) expressing cells have been suggested to be the stem cells that give rise to a Dlx2+ transiently fast amplifying neural progenitor population, which eventually generates PSA-NCAM+ neuroblasts (5). However, the placement of LeX+ or Nestin+ adult SVZ stem/progenitor cells into the current lineage model has not been carefully determined. Ependymal cells, which form a multiciliated single cell layer lining the ventricles and are in close proximity to the cells of the SVZ, were also suggested to have stem cell characteristics (6); however, subsequent studies have challenged the initial report (5, 7, 8). To date, the contribution of ependymal cells to the lineage of the postnatal SVZ still remains controversial.

Increasing evidence suggests that a number of "common" genes are shared by the stem cells of different tissue types. One of these markers, CD133 (prominin-1), has been detected in a number of stem cells, including myogenic and hematopoietic stem cells (9). CD133 expression was shown in embryonic stem cell derived neural stem cells in culture (10), putative neural stem cells of the cerebellum (11), and embryonic neuroepithelial cells (12, 13). In addition to the native stem cells, CD133 is present on numerous types of cancer stem cells, including retinoblastoma, leukemias, and brain tumors (14, 15). Collectively, CD133-immunoreactivity provides an important tool to recognize various stem cell populations.

In this study, we identified CD133 expressing cells exclusively in the postnatal ependyma. A subpopulation of ependymal cells that are CD133+ possess classical neural stem cell characteristics

in vitro and give rise to stem/progenitor cells expressing Nestin, LeX or GFAP. Furthermore, quiescent CD133+ ependymal cells *in vivo* retain the capacity for cell division and become activated upon injury. Using transplantation and genetic lineage tracing, we demonstrate that CD133+ ependymal cells generate new neurons that become part of the postnatal SVZ. Collectively, our data indicate that CD133 expressing ependymal cells render a quiescent stem cell population in the mammalian forebrain.

Results

Primary Location of the Cells Expressing CD133 in the Postnatal Forebrain.
In embryonic day (E)9, E12, and E15 telencephalon, CD133 expression was restricted to the ventricular zone (VZ) [supporting information (SI) Fig. 6 a-c]. Postnatally [i.e., postnatal day (P)0 through adulthood], CD133-immunoreactivity was localized to a "subpopulation" of the one-cell-thick layer lining the walls of the lateral ventricles, the ependyma (Fig. 1 a–e). In all cases, postnatal CD133+ cells were adjacent to the overlying SEZ and displayed a multiciliated morphology extending into the lateral ventricles—different from the single/short process bearing GFAP+ cells (Fig. 1 a–e and k). Using *in situ* hybridization, we demonstrated exclusive expression of prominin-1 mRNA in the forebrain by the ependymal cells (Fig. 1f). Furthermore, CD133+ cells were colabeled with S100β (Fig. 1i), a known—but not exclusive—marker of the ependymal cells (8). Although all of the ependymal cells were immunoreactive for β-IV tubulin—a marker that labels cilia (16)—only a subpopulation of ependymal cells was CD133+/β-IV tubulin+ (Fig. 1g). Moreover, some CD133+ ependymal cells were also immunoreactive for CD24 (SI Table 1), a surface protein that is present on some of the ependymal cells, and on the neuroblasts in the SEZ (Fig. 1h). CD133+ ependymal cells did not colocalize either with PSA-NCAM+ neuroblasts (Fig. 1j) or GFAP expressing cells (Fig. 1k) of the adult SEZ. Our findings reveal that cells expressing the stem cell marker CD133 persist throughout development and proceed into adulthood as part of the ependyma.

Stem Cell Characteristics of the Adult CD133+ Ependymal Cells *in Vitro*.
To determine whether CD133+ cells possess characteristics of neural stem cells, we microdissected and dissociated the walls

---

Fig. 1. Localization of CD133$^+$ cells in the postnatal forebrain. (*a* and *b*) Sagittal sections of adult forebrain stained with CD133 (brown) and methyl green. The RMS is outlined with dotted lines. A subpopulation of ciliated ependymal cells lining the lateral ventricle is CD133$^+$ (arrows in *b*). (Scale bars: *a*, 400 μm and *b*, 100 μm.) (*c*–*e*) Electron microscopic demonstration of the localization of CD133 to the membrane and the cilia of the ependymal cells. The section in *c* is not counterstained to demonstrate DAB depositions (arrows) on the cilia of the ependymal cells, whereas *d* shows a counterstained section to reveal subcellular structures. Note the characteristics of ependymal cells, such as lipid droplets, mirovilli, and cilia. Arrows in *e* indicate the gold particles that are concentrated on the cilia of ependymal cells. (Scale bars: *c* and *d*, 4 μm and *e*, 0.2 μm.) (*f*) Detection of prominin-1 mRNA in the ependyma by *in situ* hybridization (arrows). (Scale bar: 100 μm.) (*g*) An adult forebrain section stained with CD133 (red) and the ciliar marker β-IV tubulin (green), showing CD133$^+$/β-IV tubulin$^+$ (yellow, arrows) and β-IV tubulin$^+$/CD133$^-$ (green, arrowheads) ependymal cells. (Scale bar: 200 μm.) (*h*) Adult forebrain SVZ region immunostained with CD24 (green) and CD133 (red). Arrowheads indicate CD24$^+$ ependymal cells in the ependyma and subependyma, whereas arrows point to CD133$^+$ cells. (*Upper Inset*) CD133$^+$ ependymal cells (arrows) and a CD24$^+$ subependymal cell (arrowhead). (*Lower Inset*) CD24$^+$ ependymal and subependymal cells (arrowheads) and CD24$^+$/CD133$^+$ ependymal cells (arrows). (*i*) An adult forebrain section stained with CD133 (red) and S100β (green), showing double-stained ependymal cells (arrows). (Scale bar: 200 μm). (*j* and *k*) Fluorescent photomicrographs of representative sagittal sections obtained by confocal microscopy from adult SVZ region. CD133$^+$ ependymal cells (red) do not overlap with PSA-NCAM$^+$ neuroblasts (green in *j*) or with GFAP$^+$ cells (green in *k*) in the SEZ. The arrow in *k* points to GFAP$^+$ processes touching the ventricle that are CD133$^-$. (Scale bars: 200 μm.) CC, corpus callosum; cp, choroid plexus; ld, lipid droplet; LV, lateral ventricle; Nu, nucleus; SVZ, subventricular zone.

of the lateral ventricles into single cells from early postnatal and adult mice. CD133$^+$ cells were purified by using fluorescence-activated cell sorting (FACS). Using quantitative-RT-PCR, we demonstrated enrichment of CD133 signal in the sorted cell populations (SI Fig. 7*a*).

Sorted CD133$^+$ cells gave rise to all three lineages of the CNS, when grown and differentiated on adherent surfaces for 6–9 days (SI Fig. 7 *b-d*). When plated on uncoated surfaces at a clonal density in the presence of fibroblast growth factor (bFGF), sorted CD133$^+$ cells formed neurospheres at a 5.9% rate (Fig. 2 *a* and *d*). During the early stages of sphere development, most of the CD133$^+$ neurospheres were motile and displayed a "spinning" type of motion, a behavior associated with ependymal spheres (7, 8). Once primary spheres were dissociated and plated clonally as single cells, secondary (6.6%), tertiary (6.1%),

quaternary (6.9%), and quinary (7.2%) spheres formed, indicating that CD133$^+$ cells self-renew for prolonged time points *in vitro* (17) (Fig. 2 *b* and *d*). With each passage, CD133$^+$ cell population in neurospheres remained constant (i.e., 12.9, 13.2, and 12.1% in primary, secondary, and tertiary neurospheres, respectively) as shown by FACS analysis (Fig. 2*e*). Using RT-PCR, we detected CD133 and LeX expression from primary neurospheres at 6 days *in vitro* (DIV) under bFGF treatment (Fig. 2*f*). Note that GFAP was not expressed by the cells in the neurospheres under proliferation conditions and was up-regulated upon differentiation of primary neurospheres (Fig. 2*f*). When CD133$^+$ cell-initiated neurospheres (Fig. 2*g*) were plated on PO-Fn coated slides in the absence of bFGF, they differentiated and gave rise to neurons, astrocytes, and oligodendrocytes, demonstrating the multipotency of CD133$^+$ stem cells (Fig. 2 *h*–*j*).

In previous reports, ependymal cells were postulated to lack stem cell properties, when CD24-immunoreactivity was used to identify ependymal cells (5, 7). However, CD24 is expressed also in the PSA-NCAM$^+$ neuroblasts in the SEZ (18), making CD24 a nonspecific marker for ependymal cells. Nevertheless, to test whether CD24$^+$ cells behave as stem cells in our culture conditions, we sorted and plated CD24$^+$ cells in exactly the same way as CD133$^+$ cells. A very small percentage of CD24$^+$ cells (i.e., 0.9%) generated spheres that were smaller and did not yield any secondary spheres (Fig. 2 *c* and *d*), similar to the findings of previous studies (7, 8). Our data indicate that only CD133$^+$/CD24$^-$ ependymal cells carry stem cell potential.

Induction of Quiescent CD133$^+$ Stem Cells upon Chemical Insult/Injury. Although ependymal cells have been suggested to divide infrequently *in vivo* (5, 7), our analysis of large scale adult brain sections demonstrated occasional proliferating CD133$^+$ cells, using Ki67-immunoreactivity (Fig. 3 *a* and *b*). To test whether relatively quiescent ependymal cells can be activated *in vivo*, we injected the anti-mitotic agent Cytosine-β-D-arabinofuranoside (Ara-C) into the lateral ventricles of adult mice. Ara-C treatment selectively eliminates fast dividing cells (5) and presumably induces resident stem cells to proliferate in response. Injected animals were administered BrdU for 2 weeks. We detected CD133$^+$/BrdU$^+$ cells (Fig. 4 *c–f*), indicating that CD133 expressing ependymal cells remain "inducible" for cell division.

**Generation of New Neurons by CD133$^+$ Ependymal Stem Cells in the Adult SVZ/RMS *in Vivo*.** To determine the progeny of CD133$^+$ ependymal cells, we used Nestin/GFP transgenic mice, in which the expression of GFP is under the control of nestin (19). In these animals, Nestin/GFP expressing cells mark the postnatal SVZ and RMS very distinctly (Fig. 4*a*). Furthermore, the half life of GFP protein is longer compared with Nestin, making it possible to partially trace cells that had expressed Nestin in their lineage history. When CD133$^+$ cells were collected from Nestin/GFP mice, using FACS, virtually all of them were GFP$^-$ (Fig. 4*b*). In addition, CD133$^+$ cells were not immunoreactive for LeX, GFAP, or Nestin (Fig. 4 *c–e*). However, increasing number of GFP$^+$ green spheres that were clonally originated from CD133$^+$ ependymal neural stem cells was observed 3–7 DIV. Nestin/GFP$^+$ neurospheres also contained LeX$^+$ stem cells (Fig. 4 *f–k*).

To characterize the progeny of CD133$^+$ stem cells in the adult forebrain, we traced them *in vivo*, using a transplantation approach. Purified CD133$^+$/GFP$^-$ cells from adult Nestin/GFP mice were injected into the lateral ventricles of wild type adult animals. At the time of injections, none of the sorted CD133$^+$ cells were GFP$^+$. We observed a number of GFP$^+$ cells along the RMS 1 or 2 weeks after transplantation (Fig. 4*l*), indicating that CD133$^+$ cells integrate into the recipient tissue and produce cells destined for SVZ/RMS *in vivo*. Furthermore, none of the GFP$^+$ cells, even in the close proximity of the lateral ventricle, were
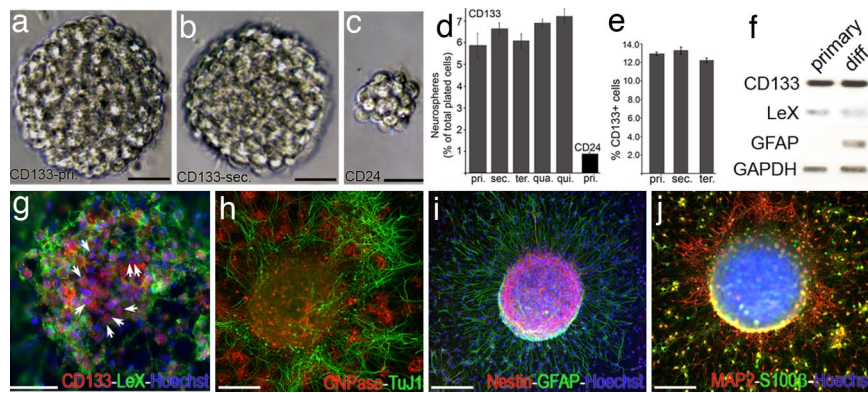
Fig. 2. Self-renewal capacity and multipotency of CD133$^+$ ependymal cells. (*a*) A representative primary neurosphere at 6 DIV that originated clonally from a CD133$^+$ ependymal cell. (Scale bar: 50 μm.) (*b*) Secondary spheres form upon dissociation of the primary neurospheres demonstrating the self-renewal capacity of CD133$^+$ cells. (Scale bar: 50 μm.) (*c*) A representative primary sphere at 6 DIV originated clonally from a CD24$^+$ ependymal cell. (Scale bar: 50 μm.) (*d*) Relative percentages of primary (pri.), secondary (sec.), tertiary (ter.), quaternary (qua.), and quinary (qui.) neurospheres originated from CD133$^+$ ependymal cells. (*e*) The percentage of CD133$^+$ ependymal cells in primary, secondary, and tertiary neurospheres at 7 DIV analyzed by FACS. (*f*) RT-PCR analysis of the expression of CD133, LeX, GFAP, and GAPDH from proliferating primary neurospheres at 6 DIV under bFGF treatment or from differentiated spheres in the absence of bFGF on coated slides for 7 days. (*g–j*) Fluorescent images taken from differentiated primary neurospheres originated from CD133$^+$ ependymal cells (arrows in *g*) 3 or 7 (*h–j*) days after they were plated on coated slides after mitogen withdrawal. CD133$^+$ neurospheres contain LeX$^+$ progenitor/stem cells, TuJ1$^+$ and MAP2$^+$ neurons, CNPase$^+$ oligodendrocytes, S100β^+ and GFAP$^+$ astrocytes, and nestin$^+$ progenitor cells, demonstrating their multipotency. (Scale bars: *g*, 50 μm and *h–i*, 100 μm.)

colabeled with CD133 (Fig. 4*m*). GFP$^+$ cells were immunoreactive for the immature neuronal marker doublecortin (Fig. 4*n*), the astrocytic—or adult stem cell—marker GFAP (Fig. 4*o*), or the proneural bHLH transcription factor Mash1 (Fig. 4*p*). Most of the GFP$^+$ cells were colocalized with PSA-NCAM$^+$ neuroblasts (Fig. 4*q*), although none of them costained with Olig2 (Fig. 4*r*).
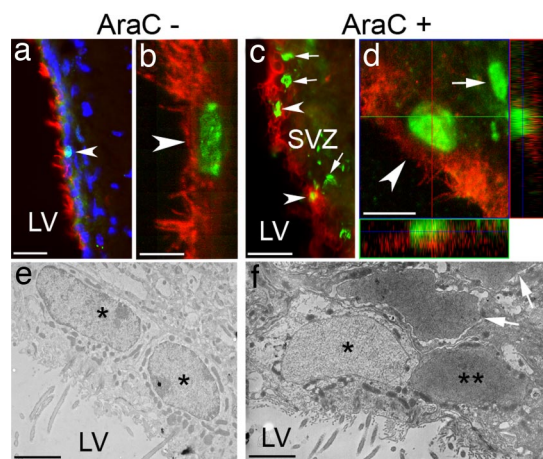

Fig. 3. Proliferation and induction of CD133$^+$ ependymal cells. (*a* and *b*) Occasional CD133$^+$ ependymal cells (red) labeled with the cell proliferation marker Ki67 (green, arrowheads) analyzed with conventional (*a*) or confocal (*b*) microscopy. (Scale bars: *a*, 100 μm and *b*, 15 μm.) (*c*) CD133$^+$ ependymal cells (red) incorporate BrdU (green) 14 days after the administration of Ara-C. Arrowheads point to BrdU$^+$ cells in the ependymal layer. Arrows indicate BrdU$^+$ cells in the SEZ. (Scale bar: 150 μm.) (*d*) A z-stack confocal analysis of a representative CD133$^+$/BrdU$^+$ cell (arrowhead). The arrow points to a BrdU$^+$/CD133$^-$ cell in the SEZ. (Scale bar: 20 μm.) (*e* and *f*) Electron microscopic analysis of BrdU$^+$ ependymal/subependymal cells upon AraC treatment. (*e*) Two BrdU$^-$ ependymal cells (asterisks). (*f*) A BrdU$^+$ ependymal cell (double asterisks) next to a BrdU$^-$ ependymal cell (asterisk). Arrows mark BrdU$^+$ cells in the SEZ. Note the similarities of the morphology of BrdU$^+$ (double asterisks) and BrdU$^-$ (asterisk) ependymal cells (e.g., shape of the nucleus, ciliated morphology, and round lipid droplets around the nuclei) and the differences between the BrdU$^+$ ependymal cell (double asterisks) and subependymal cells (arrows). LV, lateral ventricle; SVZ, subventricular zone. (Scale bars: 4 μm.)

We further examined the contribution of CD133$^+$ ependymal stem cells to the lineage of postnatal SVZ, using a genetic approach. Human CD133 analog, AC133, contains four promoters in front of alternative start sites in exon 1 (SI Fig. 8). Exon 1B is the main splice variant used in the brain under the control of the P2 promoter (20) (SI Fig. 8). We excised the mouse CD133 promoter fragment that contains the sequence homologues to the human P2 promoter (designated "mP2") and inserted it into an expression vector containing Cre-GFP fusion protein. Furthermore, in another vector, we replaced the prominin promoter—upstream of Cre-GFP—with a short 2.0-kb GFAP promoter to label postnatal GFAP$^+$ cells (5).

The specificity of mP2 and GFAP promoters were characterized *in vitro* and *in vivo*. Dissociated cells from the lateral ventricles were transfected with mP2 and GFAP promoters 1 day after plating. Analysis of GFP-Cre$^+$ cells 2 days after transfection demonstrated that mP2 minimal promoter construct was specific to CD133$^+$ cells, whereas the GFAP promoter was solely expressed by GFAP$^+$ cells (SI Fig. 9). Subsequently, mP2 or GFAP expression plasmids were injected into the lateral ventricles of wild type P3 pups, followed by electroporation to transfect cells surrounding the ventricles. Four or 7 days after injection, GFP$^+$ cells were exclusively detected in the ependymal layer and none in the SEZ (Fig. 5 *a* and *b* and SI Fig. 10 *a* and *b*). Moreover, every GFP$^+$ mP2-transfected ependymal cell was CD133$^+$ (Fig. 5*b* and SI Fig. 10*a*) and GFAP$^-$ (SI Fig. 10*b*), demonstrating the specificity of the mP2 construct *in vivo*. Unlike in the case of Nestin/GFP, where GFP is relatively long-lived, our experimental data suggest that Cre-GFP fusion protein is relatively short-lived, because we never observed any CD133$^-$ cells expressing GFP 7 days postinjection. In animals that were injected with the GFAP promoter, GFP$^+$ cells were only detected in the subependyma, and none were detected in the ependyma (SI Fig. 10 *c* and *d*). Additionally, GFAP promoter transfected cells were GFAP-immunoreactive (SI Fig. 10*c*), but none of them were CD133$^+$ (SI Fig. 10*d*). Collectively, these data indicated that electroporation of the CD133 minimal promoter allows for highly specific transgene expression in CD133$^+$ ependymal cells.

To trace the progeny of CD133$^+$ ependymal stem cells *in vivo*, we used a Rosa26-lacZ mouse reporter line that contains a
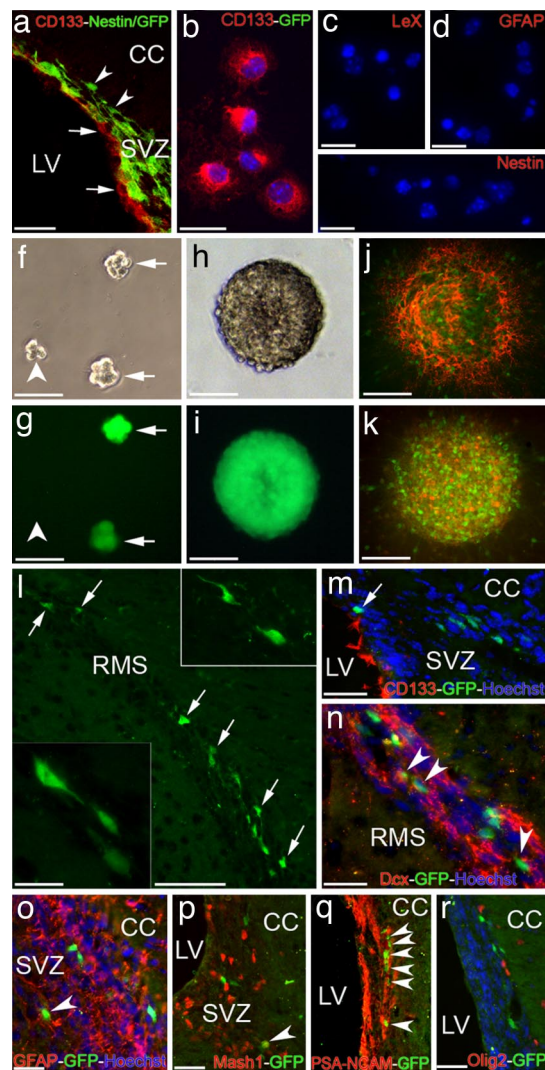
Fig. 4. Contribution of transplanted CD133+ cells to the lineage of adult SVZ. (*a*) Confocal image of the SVZ region of adult Nestin/GFP mouse, stained with anti-CD133 (red). Arrows point to CD133+ ependymal cells. Arrowheads indicate Nestin-GFP cells in the SEZ. (Scale bar: 200 μm.) (*b–e*) Sorted CD133+ cells (red) from Nestin/GFP mice are not immunoreactive for GFP, LeX, GFAP, or Nestin during the first DIV. (Scale bars: *b*, 20 μm and *c–e*, 30 μm.) (*f–i*) Clonally generated neurospheres from a CD133+ cell—isolated from Nestin/GFP mice—captured from the same area at 2 (*f* and *g*) or 6 (*h* and *i*) DIV with either bright field (*f* and *h*) or GFP (*g* and *i*) filters. Arrows point to Nestin/GFP+ spheres, whereas the arrowhead denotes a forming sphere with no GFP expression yet. (Scale bars: *f* and *g*, 75 μm and *h* and *i*, 100 μm.) (*j* and *k*) Differentiated spheres on coated surfaces at 5 DIV expressing Nestin/GFP and stained with LeX (red in *j*) or CD133 (red in *k*). (Scale bars: 100 μm.) (*l*) GFP+ cells (arrows) migrating along the RMS 2 weeks after transplantation of sorted CD133+/GFP− cells from Nestin/GFP mice into the lateral ventricles of wild-type-recipient mice. (Scale bar: 250 μm.) (*Insets*) Higher magnification of migrating GFP+ cells in the RMS. (Scale bar: 20 μm.) (*m*) A confocal photomicrograph of the SVZ region of a recipient mouse 1 week after the sorted CD133+ cells were injected into the lateral ventricle. Even in close proximity of the ventricular surface, GFP+ cells (arrow) are CD133− (red). (*n–r*) Migrating GFP+ cells (green) in the SVZ/RMS are colabeled with doublecortin (arrowheads in *n*), GFAP (arrowhead in *o*), Mash1 (arrowhead in *p*) or PSA-NCAM (arrowheads in *q*). None of the GFP+ cells are costained with Olig2 (*r*). CC, corpus callosum; LV, lateral ventricle; RMS, rostral migratory stream; SVZ, subventricular zone. (Scale bars: *n–o*, 250 μm.)
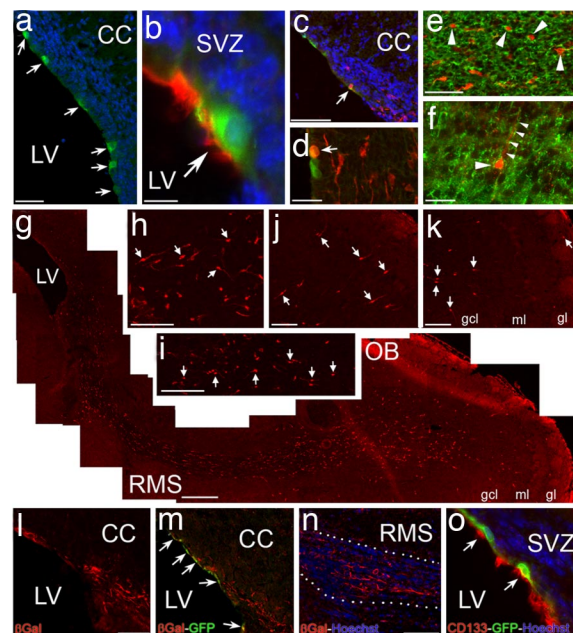
Fig. 5. Generation of olfactory bulb interneurons by CD133+ ependymal neural stem cells in the postnatal forebrain. (*a*) GFP+ cells (green) that were transfected with an expression vector plasmid containing a short prominin-1 promoter (i.e., mP2) governing Cre-GFP expression line the ventricles (arrows). (Scale bar: 150 μm.) (*b*) A GFP+ transfected cell (arrow) in the ependymal layer is also CD133+ (red). (Scale bar: 15 μm.) (*c* and *d*) Fluorescent photomicrographs taken from Rosa26 reporter mice injected with mP2 plasmid. Transfected GFP+ cells (green) are in the ependyma whereas the β-gal+ cells (red) are in the ependyma and SEZ. Arrows point to transfected ependymal cells that started to express β-gal. (Scale bar: *c*, 200 μm and *d*, 50 μm.) (*e*) β-gal+ migrating cells (red) in the RMS are PSA-NCAM+ (green, arrowheads). (Scale bar: 75 μm.) (*f*) A migrating β-gal+ cell (red) in the layers of the olfactory bulb is TuJ1+ (green, arrowhead). Small arrowheads point to the process of the β-gal+ cell extending into the overlying layer of the olfactory bulb. (Scale bar: 50 μm.) (*g*) A photomontage of a P10 Rosa26 reporter mouse forebrain showing the entire extent of the RMS and olfactory bulb in a sagittal plane. The animal was injected with the mP2 construct at P3. β-gal+ cells (red) are distributed along the RMS from SVZ to the layers of the olfactory bulb. (Scale bar: 400 μm.) (*h–k*) Localization of β-gal+ cells in the RMS (arrows in *h* and *i*) and the layers of the olfactory bulb (arrows in *j* and *k*) of a P10 Rosa-26 reporter mouse. (Scale bars: 75 μm.) (*l* and *m*) A fluorescent photomicrograph of an adult Rosa26 reporter mouse forebrain injected with mP2 construct showing the SVZ region. β-gal+ cells (red) are distributed in the ependyma and SEZ, whereas transfected GFP+ cells line the ventricles (green, arrows). (Scale bar: 200 μm.) (*n*) Localization of β-gal+ cells (red) along the RMS en route to the olfactory bulb. Dotted white line outlines the borders of the RMS. (Scale bar: 250 μm.) (*o*) GFP+ transfected cells (green) in the ependymal layer of an adult Rosa26 reporter mouse are also CD133-immunoreactive (arrows, red). Hoechst staining (blue) was used to label nuclei. (Scale bar: 75 μm.) CC, corpus callosum; gcl, granule cell layer; gl, glomerular layer; LV, lateral ventricle; ml, mitral cell layer; OB, olfactory bulb; RMS, rostral migratory stream; SVZ, subventricular zone.

"floxed" stop codon in front of a lacZ gene at the Rosa26 locus. mP2 plasmid was injected into the lateral ventricles of P3 and adult Rosa26 mice followed by electroporation. This approach allows for identification of the mP2 transfected cells, using Cre-GFP, and the progeny of the transfected cells, using β-gal. One week after the injection of mP2, we detected numerous β-gal+ cells that were PSA-NCAM+ with a typical morphology of migrating neurons in the SVZ and RMS (Fig. 5 *c–e* and *g*). Two weeks after injection, a number of β-gal+ cells that were immunoreactive for TuJ1 was located in the layers of the olfactory bulb (Fig. 5 *f–k*).

We examined mP2-transfected cells to determine the source of β-gal+ cells in the RMS of Rosa26 reporter animals. We exclusively detected GFP+ cells in the ependymal layer lining the ventricles (Fig. 5a) and none in the SEZ. Moreover, every GFP+ transfected ependymal cell was also CD133+ (Fig. 5b). Subse-

quently, the same injection protocol was repeated by using adult Rosa26 reporter mice. We again detected GFP$^+$ cells in the ependymal layer—and none in the SEZ—(Fig. 5m) and β-gal$^+$ cells along the RMS 2–4 weeks after injection (Fig. 5 l–n). In addition, every GFP$^+$ transfected ependymal cell was also CD133$^+$ (Fig. 5o), indicating that the proliferation capacity of CD133$^+$ ependymal cells is not restricted to neonatal period. Note that electroporation by itself does not reactivate ependymal stem cells (data not shown). Collectively, our transplantation and genetic tracing experiments in neonatal and adult mice demonstrate the *in vivo* stem cell activity of CD133$^+$ ependymal cells and their contribution to the lineage of postnatal SVZ.

Discussion

Work over the last decade revealed that neural stem cells persist in the adult mammalian forebrain and generate new neurons throughout life, but the nature of these stem cells is incompletely understood. CD133 is a broadly accepted marker for stem cells, including neural stem cells (15). However, the location and identity of CD133 expressing cells in the mammalian brain remain elusive. In this study, we reveal that a subpopulation of adult ependymal cells, expressing CD133, fulfills the criteria of bona fide neural stem cells *in vivo* and *in vitro*. Furthermore, we show that ependymal cells expressing CD24 (regardless of whether they also express CD133 or not) do not exhibit stem cell characteristics, which may explain why previous studies that used CD24 to identify ependymal stem cells had reached the conclusion that the ependyma does not contain neural stem cells.

More than One Neural Stem Cell Population in the Adult CNS. We demonstrate that the cells expressing the stem cell marker CD133 belong to a subpopulation of postnatal ependymal cells. Although our data do not argue against the observation that GFAP$^+$ and/or LeX$^+$ subependymal cells also fulfill the current neural stem cell criteria, we propose that CD133$^+$ ependymal cells represent a more quiescent neural stem cell population that is upstream of GFAP and/or LeX expressing cells. Furthermore, our data do not exclude the possibility of GFAP$^+$ or LeX$^+$ cells reciprocally giving rise to CD133$^+$ ependymal stem cells. The presence of more than one type of stem cell in a particular system is well established. For example, the hematopoietic system contains both long-term and short-term stem cells (21), whereas, in the mammalian skin, two types of epithelial stem cells are present (22). Thus, it is plausible that the adult nervous system may also contain different types of stem cells.

Quiescent Adult Neural Stem Cells. In agreement with reports that described the quiescence of ependymal cells (5, 7, 23), we also found that CD133$^+$ ependymal cells are more quiescent compared with GFAP$^+$ subependymal cells. However, our data indicate that the ependyma is not 100% postmitotic. Occasionally, CD133$^+$ cells in a mitotic cycle (i.e., Ki67$^+$) could indeed be detected in the ependyma. Additionally, in response to anti-mitotic drugs, increased activation of mitotic features in the CD133$^+$ependymal cells can be observed. It has been reported that ependymal cells originate from embryonic radial glial cells that are generally considered as the multipotent neural stem cells in embryonic stages (23). Although the same report postulated that ependymal cells were absolutely postmitotic, the negative data do not preclude the possibility that some quiescent neural stem cells (e.g., radial glial cells) in the developing embryos may preserve their quiescence into adult stages when they become ependymal cells.

Our *in vitro* stem cell assays and *in vivo* transplantation experiments indicate that CD133$^+$ ependymal cells satisfy all of the criteria of a bona fide neural stem cell. More importantly, our genetic-lineage tracing experiments and BrdU and Ki67 labeling results clearly demonstrate that the adult ependyma is not 100%

postmitotic and that ependymal cells give rise to olfactory bulb interneurons on a regular basis. It is possible that differences in mouse strains and age and analytic approaches can increase or decrease the detectability of mitotic figures in the ependyma.

The ''Neurogenic Niche'' and the ''Neural Stem Cell Niche.'' Because CD133$^+$ ependymal cells are constantly in contact with the cerebrospinal fluid (CSF), we propose that the CSF supports a potential neural stem cell niche for the adult SVZ, which leads neural stem cells to temporarily withdraw from the cell cycle and enter a quiescent state (see SI Fig. 11 and *SI Text* for details). In the adult, Notch signaling is active in the ependyma, which might be involved in maintaining neural stem cells in an undifferentiated quiescent state (6). Inhibition of this pathway might be involved in stem cell activation. Consistently, in the developing cerebral cortex, it has been shown that CD133$^+$/Notch^{high} cells display neural stem cell features, whereas Notch^{low} cells are actively involved in neurogenesis (24).

In recent years, rapid proliferation capability has been regarded as representative for ''stemness'' in neural stem cells. As a result, it is generally believed that the neural stem cell niche should contain activities that enhance proliferation and neurogenic potential of stem cells. We propose that such a niche should be more appropriately referred to as the neurogenic niche. In the field of neural stem cell research, the neurogenic niche has often been used interchangeably with the neural stem cell niche, which is rather misleading. We suggest that similar to stem cell niches in other systems, the neural stem cell niche should be involved in maintaining stem cells in a multipotent, and mitotically, and metabolically quiescent state, thus preserving the stem cells. It is worth noting that CD133$^+$ ependymal cells are also located in the third and fourth ventricles and the central canal of the spinal cord (SI Fig. 6). Although these cells may still contain stem cell properties, because of the lack of a neurogenic niche, they do not produce new neurons on a regular basis. Because ≈6% of the CD133$^+$ cells form neurospheres, we cannot exclude the possibility that not all CD133$^+$ cells (e.g., CD133$^+$/CD24$^+$) are stem cells. The quiescent nature of CD133$^+$ ependymal cells makes them more comparable with the stem cells found in other systems, such as skin stem cells (22) and *Drosophila* germ-line stem cells (25), than do the previously postulated adult neural stem cell populations (GFAP$^+$ and/or LeX$^+$ cells). Although CD133$^+$ cells can give rise to fast-proliferating progeny, our finding that CD133$^+$ neural stem cells are normally quiescent ependymal cells *in vivo* suggests that the nervous system, similar to other systems, harbors multipotent quiescent stem cells, and that the previously identified neural stem cells in adult brain may represent a more downstream cell population.

Materials and Methods

Surgery. Neonatal and adult mice were transcardially perfused by using 4% PFA. All brains were processed as described in ref. 26. Using stereotaxic coordinates, dissociated cells or plasmid DNA constructs were injected into the lateral ventricles, followed by electroporation. Details of surgical procedures are provided in *SI Text*.

Cell Culture. A modified protocol was used to culture postnatal SVZ cells (26). Dissociated cells were isolated by using FACS. For a detailed description, see *SI Text*.

Immunostaining, *in Situ* Hybridization, EM. Analyses were performed as described in ref. 26. For a detailed description, see *SI Text*.

Promoter Constructs and Transfection. Mouse prominin-1 promoter or the 2.0-kb GFAP promoter was subcloned into the pGL3B (Promega) containing Cre-GFP fusion. mP2 and GFAP constructs were used in conjunction with electroporation or *in vitro*.

1. Luskin MB (1993) *Neuron* 11:173–189.
2. Lois C, Alvarez-Buylla A (1994) *Science* 264:1145–1148.
3. Gage FH (2000) *Science* 287:1433–1438.
4. Coskun V, Luskin MB (2001) *J Neurosci* 21:3092–3103.
5. Doetsch F, Caille I, Lim DA, Garcia-Verdugo JM, Alvarez-Buylla A (1999) *Cell* 97:703–716.
6. Johansson CB, Momma S, Clarke DL, Risling M, Lendahl U, Frisen J (1999) *Cell* 96:25–34.
7. Capela A, Temple S (2002) *Neuron* 35:865–875.
8. Chiasson BJ, Tropepe V, Morshead CM, van der Kooy D (1999) *J Neurosci* 19:4462–4471.
9. Miraglia S, Godfrey W, Yin AH, Atkins K, Warnke R, Holden JT, Bray RA, Waller EK, Buck DW (1997) *Blood* 90:5013–5021.
10. Kania G, Corbeil D, Fuchs J, Tarasov KV, Blyszczuk P, Huttner WB, Boheler KR, Wobus AM (2005) *Stem Cells* 23:791–804.
11. Lee A, Kessler JD, Read TA, Kaiser C, Corbeil D, Huttner WB, Johnson JE, Wechsler-Reya RJ (2005) *Nat Neurosci* 8:723–729.
12. Marzesco AM, Janich P, Wilsch-Brauninger M, Dubreuil V, Langenfeld K, Corbeil D, Huttner WB (2005) *J Cell Sci* 118:2849–2858.
13. Uchida N, Buck DW, He D, Reitsma MJ, Masek M, Phan TV, Tsukamoto AS, Gage FH, Weissman IL (2000) *Proc Natl Acad Sci USA* 97:14720–14725.
14. Reya T, Morrison SJ, Clarke MF, Weissman IL (2001) *Nature* 414:105–111.
15. Singh SK, Hawkins C, Clarke ID, Squire JA, Bayani J, Hide T, Henkelman RM, Cusimano MD, Dirks PB (2004) *Nature* 432:396–401.
16. Renthal R, Schneider BG, Miller MM, Luduena RF (1993) *Cell Motil Cytoskeleton* 25:19–29.
17. Reynolds BA, Rietze RL (2005) *Nat Methods* 2:333–336.
18. Calaora V, Chazal G, Nielsen PJ, Rougon G, Moreau H (1996) *Neuroscience* 73:581–594.
19. Yamaguchi M, Saito H, Suzuki M, Mori K (2000) *Neuroreport* 11:1991–1996.
20. Shmelkov SV, Jun L, St Clair R, McGarrigle D, Derderian CA, Usenko JK, Costa C, Zhang F, Guo X, Rafii S (2004) *Blood* 103:2055–2061.
21. Morrison SJ, Uchida N, Weissman IL (1995) *Annu Rev Cell Dev Biol* 11:35–71.
22. Blanpain C, Lowry WE, Geoghegan A, Polak L, Fuchs E (2004) *Cell* 118:635–648.
23. Spassky N, Merkle FT, Flames N, Tramontin AD, Garcia-Verdugo JM, Alvarez-Buylla A (2005) *J Neurosci* 25:10–18.
24. Mizutani K, Yoon K, Dang L, Tokunaga A, Gaiano N (2007) *Nature* 449:351–355.
25. Lin H (2002) *Nat Rev Genet* 3:931–940.
26. Ge W, He F, Kim KJ, Blanchi B, Coskun V, Nguyen L, Wu X, Zhao J, Heng JI, Martinowich K, *et al.* (2006) *Proc Natl Acad Sci USA* 103:1319–1324.